# Supporting Information

## Wen et al. 10.1073/pnas.1601519113

### SI Materials and Methods

MD simulations of the DAFP-1 model and the X-ray structure of TmAFP (1.4-Å resolution) (52) were performed. The MD simulations were carried out using the NAMD 2.5 program (55) with the AMBER99 force field (56). The DAFP-1 model and the X-ray structure of TmAFP were neutralized by adding one and two $Na^+$ counter ions and solvated in a TIP3P (57) water box with an 18-Å buffer distance between the wall of the water box and the nearest solute atom, respectively. After initial energy minimization and heating, each system was then simulated for 10 ns of NPT dynamics at 1 bar and 277 K. The coordinates were saved every 1 ps. The trajectory files were analyzed using the visual molecular dynamics (VMD) program (58). The RMSD values of the backbone atoms (N, Cα, and C) were calculated for both DAFP-1 and TmAFP relative to their initial coordinates in the MD simulations, and the calculated RMSD values are plotted as a function of time (Fig. S3). The backbone RMSD values range from 0.3 to 0.9 Å for both DAFP-1 and TmAFP (Fig. S3), reflecting inherent protein structural flexibility and experimental resolution limits. Moreover, the structure of the DAFP-1 model and the average structure of TmAFP in the simulation are compared by aligning the Cα coordinates of the two structures (Fig. S4). The resulting RMSD is small (0.5 Å), suggesting a high backbone structural similarity between the two structures.

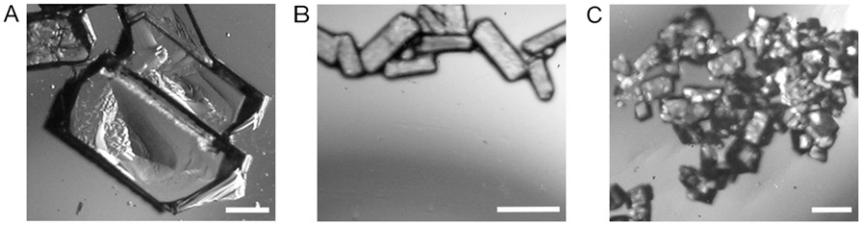


**Fig. S1.** Micrographs of trehalose dihydrate crystals. (*A*–*C*) Trehalose dihydrate crystals achieved in the absence and presence of additives. The trehalose dihydrate crystals obtained in the presence of denatured DAFP-1 at 1 mg/mL (*A*), in the presence of DAFP-1 at 0.1 mg/mL (*B*), and in the presence of DAFP-1 at 0.8 mg/mL (*C*). (Scale bars, 500 μm.)

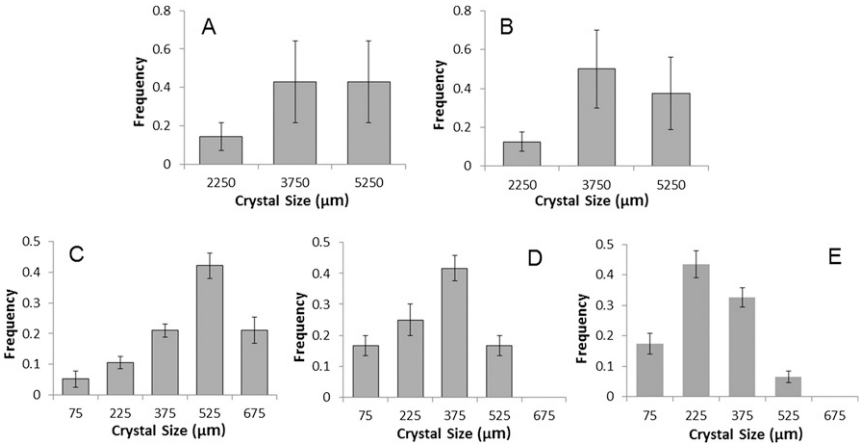


**Fig. S2.** Size distributions of trehalose dihydrate crystals in the absence and presence of varying concentrations of DAFP-1. Crystal size distributions of the achieved trehalose dihydrate crystals (*A*) in the absence of additives, (*B*) in the presence of the denatured DAFP-1 at 1.1 mg/mL (as a control), (*C*) in the presence of DAFP-1 at 0.04 mg/mL, (*D*) in the presence of DAFP-1 at 0.1 mg/mL, and (*E*) in the presence of DAFP-1 at 0.8 mg/mL. Counting errors from five experiments are represented by the error bars.

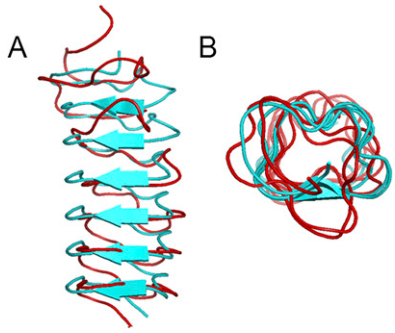


**Fig. S3.** Structural alignment of the DAFP-1 and the denatured DAFP-1 models. All of the disulfide bonds were reduced in the denatured DAFP-1 model. Structures are aligned based on backbone atoms and shown in a cartoon representation. Side view (*A*) and top view (*B*) of aligned DAFP-1 (blue) and the denatured DAFP-1 (red).

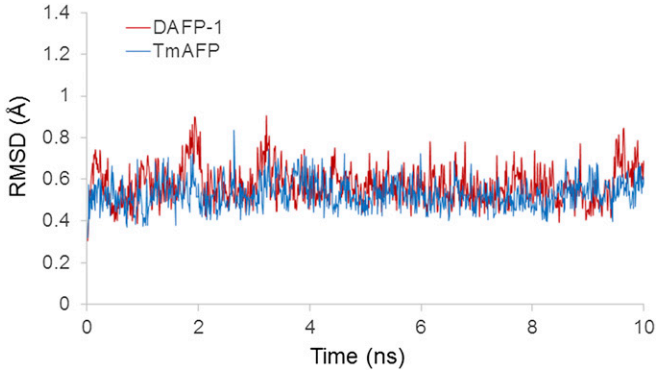


**Fig. S4.** RMSDs of all backbone atoms of DAFP-1 (red) and TmAFP (blue) as a function of simulation time. The RMSDs were calculated with respect to the initial coordinates in the simulations.

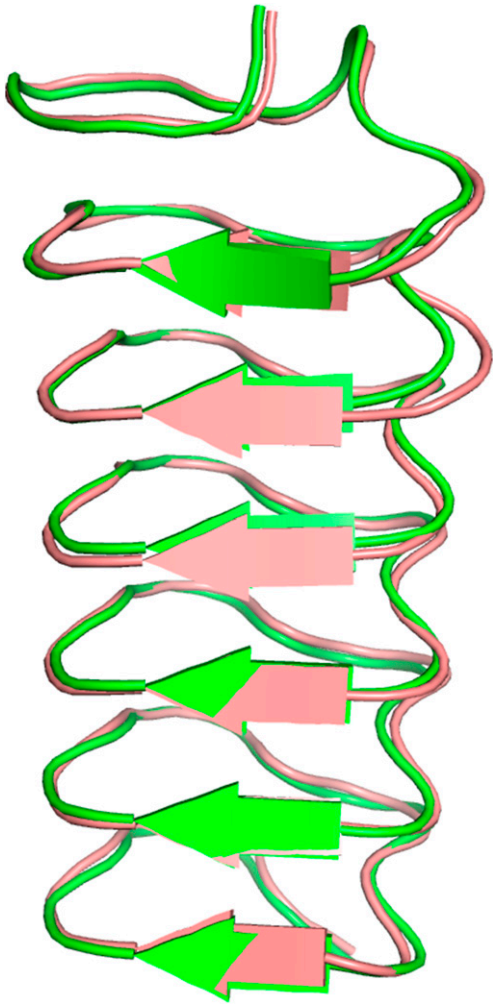

**Fig. S5.** Structural alignment of the DAFP-1 model and the average TmAFP structure from the MD simulation. The structures are aligned based on the backbone atoms and shown in a cartoon representation. The aligned DAFP-1 model and the TmAFP are shown in pink and green, respectively.

**Table S1. Crystallographic data for trehalose dihydrate**

| Crystallographic variable | Data |
|---|---|
| Formula | $C_{12}H_{22}O_{11}{\cdot}2H_2O$ |
| Formula weight | 378.33 |
| Data collection temperature | 100 K |
| Crystal system | Orthorhombic |
| Space group | $P2_12_12_1$ (#19) |
| Unit cell dimensions | |
| *a*, *b*, *c* (Å) | 7.5341 (4), 12.1764 (7), 17.7886 (10) |
| α, β, γ (°) | 90°, 90°, 90° |
| Volume | 1,631.89 (16) Å$^3$ |
| Z | 4 |
| Density (calculated) | 1.540 g/cm$^3$ |
| Reflections > 2σ(I) | 15,934 |
| Average σ (I)/(net I) | 0.0299 |
| Data/restraints/parameters | 17,593/0/330 |
| Final *R* indices [I > 2σ(I)] | $R_1 = 0.0312$, $wR_2 = 0.0596$ |
| *R* indices (all data) | $R_1 = 0.0379$, $wR_2 = 0.0602$ |

Only the data for the crystals obtained in the presence of DAFP-1 are listed, confirming that the obtained crystals are trehalose dihydrate crystals.

**Table S2. Surface energies for (−110) and (0–11) surfaces of trehalose dihydrate and the relative binding energies of DAFP-1 to these surfaces**

| Surface | $E_{surf}$ (mJ/m$^2$) | System | $\Delta\Delta E_{bind}$ (kcal/mol) | $E'_{surf}$ (mJ/m$^2$) |
|---|---|---|---|---|
| (−110) | 3,086 | DAFP-1 + (−110) | −116 | 1,825 |
| (0–11) | 2,976 | DAFP-1 + (0–11) | −75 | 1,692 |

**Table S3. Possible hydrogen bonding interactions between DAFP-1 and the crystalline surfaces of trehalose dihydrate (−110) and (0–11)**

| DAFP-1 + (−110) | | DAFP-1 + (0–11) | |
|---|---|---|---|
| DAFP-1 | (−110) | DAFP-1 | (0–11) |
| T3 O | TEL174 O14 | T3 O | TEL258 O38 |
| T26 O | TEL239 O40 | T16 O | TEL258 O40 |
| T29 O | WAT518 O | T51 O | TEL206 O38 |
| T39 O | TEL250 O28 | T53 O | TEL242 O38 |
| T41 O | WAT518 O | R54 Nη2 | TEL278 O40 |
| T51 O | TEL250 O16 | K62 Nζ | TEL170 O38 |
| T51O | TEL250 O14 | T63 O | TEL206 O40 |
| R54 Nη2 | TEL170 O16 | T65 O | TEL242 O40 |
| R54 Nε | TEL170 O16 | | |
| K62 Nζ | WAT669 O | | |
| T63 O | TEL250 O16 | | |
| T65 O | WAT513 O | | |
| T77 O | WAT510 O | | |

## Other Supporting Information Files

Dataset S1 (XLSX)
Dataset S2 (XLSX)